1

Introduction

1.1 Background

In 2004, Ander Geim and Konstantin Novoselov from the University of Manchester, UK, first obtained graphene sheets by mechanical exfoliation method, successfully fabricated the first graphene field effect transistor (FET), and investigated its unique physical properties [1]. Before the discovery of graphene, according to the thermodynamic fluctuation law, the two-dimensional (2D) atomic thick layer under nonabsolute zero degrees is unlikely to exist stably [2]. Why is graphene stable at temperatures above absolute zero? Further theoretical studies have shown that this is because large-scale graphene is not distributed in a perfect 2D plane but in a wave-like shape. The experimental results support this view [3, 4]. Therefore, the discovery of graphene shocked the condensed matter physics community and also quickly ignited the enthusiasm of scientists to study 2D materials (a crystalline material composed of a single atomic layer or few atomic layers), indicating the arrival of the "two-dimensional material era."

In 2010, Ander Geim and Konstantin Novoselov were awarded the Nobel Prize in Physics for their outstanding contribution to graphene (Figure 1.1) [1]. Graphene is a 2D material composed of carbon atoms and having a hexagonal lattice structure. Graphene has good toughness and its Young's modulus can theoretically reach as 1 TPa [5]. Therefore, graphene can form different structures through different curved stacks, such as zero-dimensional fullerenes, one-dimensional carbon nanotubes, and three-dimensional stacked graphite [6].

Graphene has shown many excellent physical properties resulting from the unique structure, and the disappearance of interlayer coupling makes the two carbon atoms in the cell completely equivalent, thus making the effective mass of electrons on the Fermi surface zero [7–11]. Because graphene has a unique Dirac band structure, carriers can completely tunnel in graphene, and electrons and holes in graphene have a very long free path. Therefore, the electronic transport of graphene is hardly affected by phonon collisions and temperature [8].

Two-Dimensional Semiconductors: Synthesis, Physical Properties and Applications,
First Edition. Jingbo Li, Zhongming Wei, and Jun Kang.

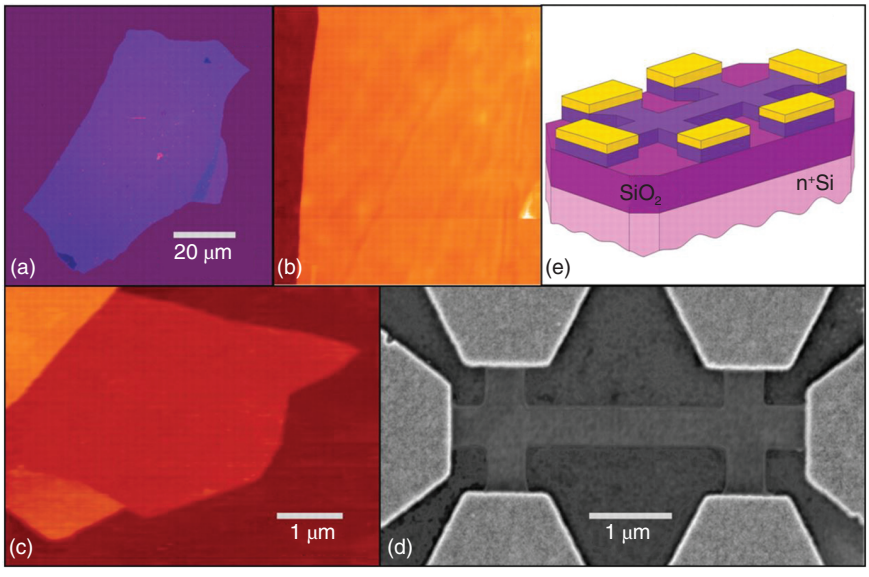

Figure 1.1 Graphene films. (a) Photograph (in normal white light) of a relatively large multilayer graphene flake with thickness ~3 nm on top of an oxidized Si wafer. (b) Atomic force microscope (AFM) image of 2 μm by 2 μm area of this flake near its edge. Colors: dark brown, SiO_2 surface; orange, 3 nm height above the SiO_2 surface. (c) AFM image of single-layer graphene. Colors: dark brown, SiO_2 surface; brown-red (central area), 0.8 nm height; yellow-brown (bottom left), 1.2 nm; orange (top left), 2.5 nm. Notice the folded part of the film near the bottom, which exhibits a differential height of ~0.4 nm. (d) SEM micrograph of an experimental device prepared from few-layer graphene, and (e) its schematic view. Source: Reproduced with permission from Novoselov et al. [1]. Copyright 2004, The American Association for the Advancement of Science.

The mobility of electrons in monolayer graphene is much larger than that in its parent graphite (Figure 1.2c) [16]. In addition, graphene has shown good thermal conductivity (Figure 1.2d) [17], room temperature quantum Hall effect (Figure 1.2a) [12, 14], single-molecule detection (Figure 1.2b), and high light transmission [18]. Graphene is a semimetal material without band gap, it cannot form a good switching ratio in terms of regulation, thus greatly limiting the application of graphene in electronic devices. Although on the bilayer and multilayer graphene, the graphene can obtain a certain band gap by applying an electric field and stress [19]. However, this band gap is not only small but also has a low electrical on/off ratio and is difficult to apply to a controllable device. With the extensive research on two-dimensional materials, it is found that the disadvantages of graphene are compensated for in other families of 2D materials [20–26].

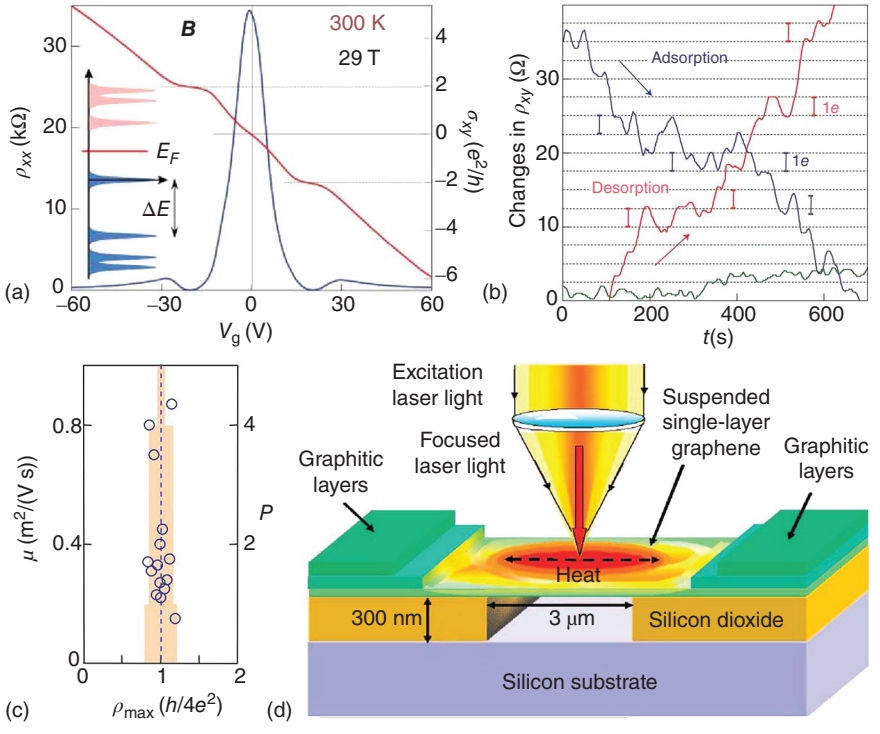

Figure 1.2 (a) Room temperature quantum Hall effect in graphene. σ_{xy} (red) and ρ_{xx} (blue) as a function of gate voltages (V_g) in a magnetic field of 29 T. The need for high B is attributed to broadened Landau levels caused by disorder, which reduces the activation energy. Source: Reproduced with permission from Novoselov et al. [12]. Copyright 2007, The American Association for the Advancement of Science. (b) Single-molecule detection in graphene. Examples of changes in Hall resistivity observed near the neutrality point ($|n| < 10^{11}$ cm^{-2}) during adsorption of strongly diluted NO_2 (blue curve) and its desorption in vacuum at 50 °C (red curve). The green curve is a reference – the same device thoroughly annealed and then exposed to pure He. The curves are for a three-layer device in $B = 10$ T. The adsorbed molecules change the local carrier concentration in graphene one by one electron, which leads to step-like changes in resistance. The achieved sensitivity is due to the fact that graphene is an exceptionally low-noise material electronically. Source: Reproduced with permission from Schedin et al. [13]. Copyright 2007, Nature Publishing Group. (c) Mobility of graphene. Maximum values of resistivity $\rho = 1/\sigma$ (circles) exhibited by devices with different mobilities μ (left y axis). The histogram (orange background) shows the number P of devices exhibiting ρ_{max} within 10% intervals around the average value of $\sim h/4e^2$. Several of the devices shown were made from two or three layers of graphene, indicating that the quantized minimum conductivity is a robust effect and does not require "ideal" graphene. Source: Reproduced with permission from Novoselov et al. [14]. Copyright 2005, Nature Publishing Group. (d) Schematic of the experiment showing the excitation laser light focused on a graphene layer suspended across a trench. The focused laser light creates a local hot spot and generates a heat wave inside single-layer graphene propagating toward heat sinks. Source: Reproduced with permission from Balandin et al. [15]. Copyright 2008, American Chemical Society.

1.2 Types of 2D Materials

The rapid pace of progress in graphene and the methodology developed in synthesizing ultrathin layers have led to exploration of other 2D materials, such as monolayer of group IVA elements (silicon, germanium, and tin) [27, 28] and their adjacent group elements (such as boron and phosphorus) monolayers; 2D layered metal oxides or metal hydroxides (octahedral or orthogonal tetrahedral structure in the layer) [29]; transition metal dichalcogenides (TMDCs) [21]; and graphene analogs such as boron nitride (BN) [30]. These 2D materials ranging from insulators (e.g. BN), semiconductors (e.g. TMDCs, tellurene, $PtSe_2$, and BP) to semimetals (e.g. $MoTe_2$), topological insulators (e.g. Bi_2Se_3), superconductors ($NbSe_2$), and metals (1T-VS_2) exhibit diverse property.

There are many 2D materials, and some literature studies have classified the 2D materials based on their positions in periodic table of elements (Figure 1.3a) [22], stoichiometric ratios [31], space groups, and structural similarities [32]. The advantage of classifying 2D materials by periodic table of elements is that 2D materials with the same group of elements often have similar properties, which has a good guiding significance for finding novel 2D materials. In 2017, Michael Ashton et al. have found that 826 2D materials can be grouped according to their stoichiometric ratios and 50% of the layered materials are represented by just five stoichiometries (Figure 1.3b) [31]. The advantage of classifying two-dimensional materials by stoichiometric ratios is to distinguish 2D materials with different stoichiometric ratios but the same elements. At the same time, when synthesizing 2D materials, the vapor pressure of growth can be adjusted according to the stoichiometric ratios, which is conductive to synthetic materials. Recently, Nicolas Mounet et al. developed a system based on high-throughput computational exfoliation of 2D materials (Figure 1.3c) [32]. They searched for materials with layered structure from more than 100 000 kinds of three-dimensional compounds in the existing database, and the 1036 kinds of easily exfoliable cases provide novel structural prototypes and simple ternary compounds by high-throughput calculations. They classify the 2D materials of the easily exfoliated group into different prototypes, according to their space groups and their structural similarities. The structure of 2D materials can be useful to search for more suitable substrates. 2D materials with a similar structure can often form stable 2D alloys. In this book, we will focus on the electronic structure, synthesis, and applications of 2D materials. We will classify 2D materials into three types based on the synthesis, structure, and application: 2D single, doped components, and van der Waals heterostructures.

2D single materials, such as graphene and MoS_2, generally refer to materials that can be exfoliated from corresponding van der Waal layered three-dimensional materials. 2D doped materials include adsorption, intercalation, substitution doping, and so on. In this book, we focus on the substitution doping: transition metal element or chalcogen element is substituted by other element, such as $MoS_{2(1-x)}Se_{2x}$ [33] and Fe-doped SnS_2 [34]. 2D heterostructures contain vertical and lateral types (Figure 1.4).

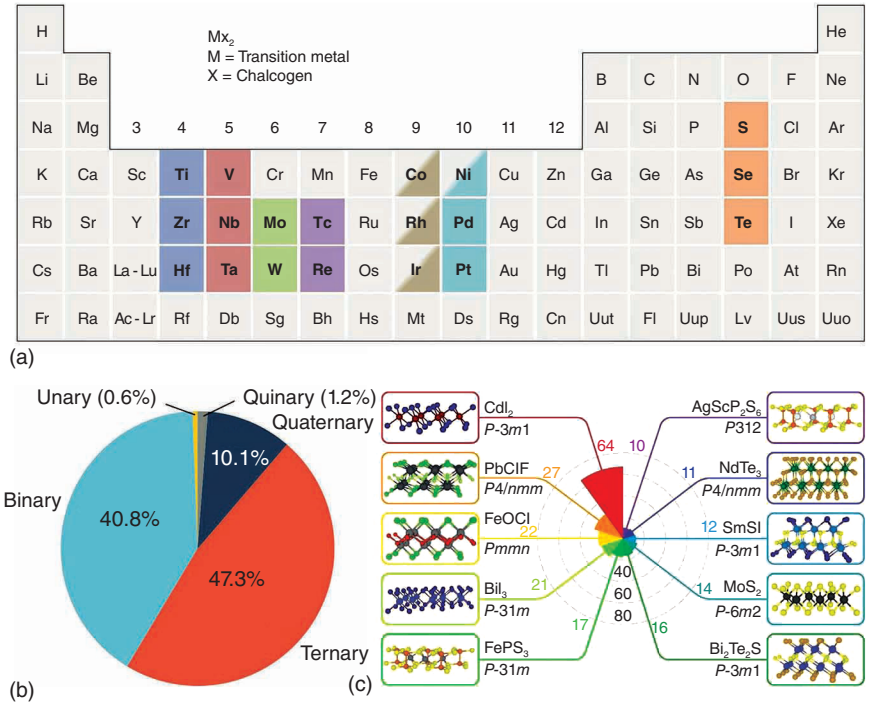

Figure 1.3 Classification of 2D materials. (a) About 40 different layered TMDCs compounds exist. The transition metals and the three chalcogen elements that predominantly crystallize in those layered structure are highlighted in the periodic table. Source: Reproduced with permission from Chhowalla et al. [22]. Copyright 2013, Nature Publishing Group. (b) Distribution of stoichiometries of the 826 layered compounds. Source: Reproduced with permission from Ashton et al. [31]. Copyright 2017, American Physical Society. (c) Polar histogram showing the number of structures belonging to the 10 most common 2D structural prototypes in the set of 1036 easily exfoliable 2D materials. A graphical representation of each prototype is shown, together with the structure-type formula and the space group of the 2D systems. The room temperature values of the thermal conductivity in the range $\sim(4.84 \pm 0.44) \times 10^3$ to $(5.30 \pm 0.48) \times 10^3$ W/mK were extracted for a single-layer graphene from the dependence of the Raman G peak frequency on the excitation laser power and independently measured G peak temperature coefficient. Source: Reproduced with permission from Mounet et al. [32]. Copyright 2018, Springer Nature.

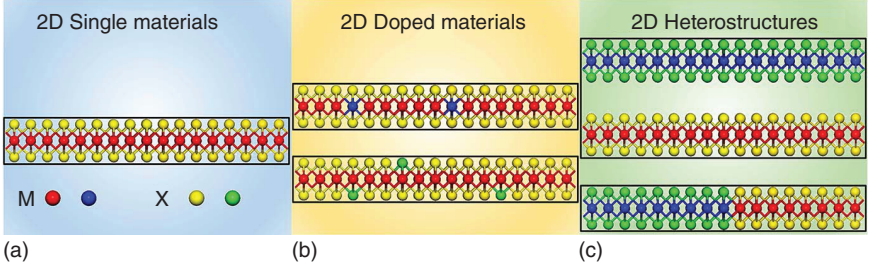

Figure 1.4 Atomic structure of (a) 2D single materials, (b) 2D doped materials, and (c) 2D heterostructures. Red and blue balls stand for transition metal element (M), yellow and green balls represent chalcogen element (X).

1.3 Perspective of 2D Materials

2D materials have been attracting wide interest because of their peculiar structural properties and fascinating applications in the areas of electronics, optics, magnetism, biology, and catalysis. Overall, the current research on 2D materials is mainly in two aspects: (i) Wafer-scale growth of 2D materials and their industrial applications. (ii) Synthesis of novel 2D materials and study their physicochemical properties.

The ability to grow large, high-quality single crystals for 2D components is essential for the industrial application of 2D devices. Until now, some 2D materials, such as MoS_2 (Figure 1.5a), WS_2 (Figure 1.5b), InSe (Figure 1.5c), and BN (Figure 1.5d), have been synthesized as wafer scale by vapor-phase deposition or pulsed laser deposition method. Thus, developing a simple and low-cost method to synthesize wafer-scale 2D materials is a current research focus. On the other hand, taking advantage of unique characteristics of 2D materials, direct integration based on 2D heterostructures is an ingenious method (Figure 1.5e) [39].

Although some 2D materials have been synthesized and investigated now, there are more than 1000 2D materials in theory and many of them still have a lot to discover, which are suggested to have peculiar property and need further study. The efforts on exploiting the application of 2D materials in optoelectronic and

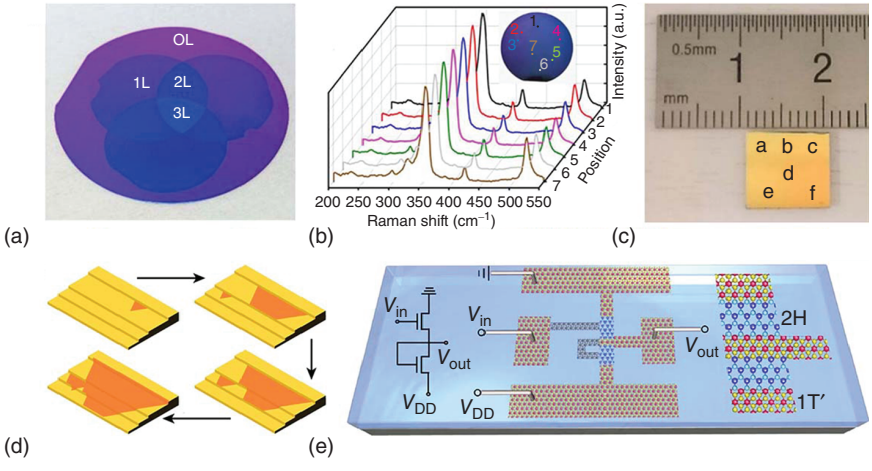

Figure 1.5 Wafer-scale growth and integrated circuit of 2D materials. (a) Three wafer-scale MoS_2 films transferred and stacked on a 4 in. SiO_2/Si wafer. Source: Reproduced with permission from Yu et al. [35]. Copyright 2017, American Chemical Society. (b) Raman spectra of WS_2 at different positions marked in the wafer-scale monolayer image. Source: Reproduced with permission from Chen et al. [36]. Copyright 2019, American Chemical Society. (c) Photograph of 1×1 cm SiO_2/Si covered with InSe film. Source: Reproduced with permission from Yang et al. [37]. Copyright 2017, American Chemical Society. (d) Schematic diagrams highlighting the unidirectional growth of h-BN domains and the anisotropic growth speed on a Cu surface with steps. This method obtained 100-cm^2 single-crystal hexagonal boron nitride monolayer on copper. Source: Reproduced with permission from Wang et al. [38]. Copyright 2019, Springer Nature. (e) Illustration of a chemically synthesized inverter based on $MoTe_2$. Source: Reproduced with permission from Zhang et al. [39]. Copyright 2019, Springer Nature.

electronic area, such as FET and photodetector, have been intensified in recent years. Multifunctional thermoelectric, superconducting, and magnetic devices need further investigation. For example, thermoelectric applications of 2D p–n junctions have not been thoroughly investigated yet. Giant magnetoresistance effect has been realized in CrI_3, while spin–orbit torque switching, spin Hall effect in antiferromagnets, and memory transistor based on 2D materials are rarely reported.

References

1 Novoselov, K.S., Geim, A.K., Morozov, S.V. et al. (2004). *Science* 306: 666.
2 Lev Davidovich, L. (1937). *Phys. Z. Sowjetunion* 11: 26.
3 Geim, A.K. and Novoselov, K.S. (2007). *Nat. Mater.* 6: 183.
4 Meyer, J.C., Geim, A.K., Katsnelson, M.I. et al. (2007). *Nature* 446: 60.
5 Lee, C., Wei, X.D., Kysar, J.W., and Hone, J. (2008). *Science* 321: 385.
6 Neto, A.C., Guinea, F., and Peres, N.M. (2006). *Phys. World* 19: 33.
7 Das Sarma, S., Adam, S., Hwang, E.H., and Rossi, E. (2011). *Rev. Mod. Phys.* 83: 407.
8 Neto, A.C., Guinea, F., Peres, N.M. et al. (2009). *Rev. Mod. Phys.* 81: 109.
9 Wallace, P.R. (1947). *Phys. Rev.* 71: 622.
10 McClure, J.W. (1957). *Phys. Rev.* 108: 612.
11 Slonczewski, J.C. and Weiss, P.R. (1958). *Phys. Rev.* 109: 272.
12 Novoselov, K.S., Jiang, Z., Zhang, Y. et al. (2007). *Science* 315: 1379.
13 Schedin, F., Geim, A.K., Morozov, S.V. et al. (2007). *Nat. Mater.* 6: 652.
14 Novoselov, K.S., Geim, A.K., Morozov, S. et al. (2005). *Nature* 438: 197.
15 Balandin, A.A., Ghosh, S., Bao, W. et al. (2008). *Nano Lett.* 8: 902.
16 Bolotin, K.I., Sikes, K., Jiang, Z. et al. (2008). *Solid State Commun.* 146: 351.
17 Balandin, A.A. (2011). *Nat. Mater.* 10: 569.
18 Nair, R.R., Blake, P., Grigorenko, A.N. et al. (2008). *Science* 320: 1308.
19 Zhang, Y.B., Tang, T.T., Girit, C. et al. (2009). *Nature* 459: 820.
20 Radisavljevic, B., Radenovic, A., Brivio, J. et al. (2011). *Nat. Nanotechnol.* 6: 147.
21 Wang, Q.H., Kalantar-Zadeh, K., Kis, A. et al. (2012). *Nat. Nanotechnol.* 7: 699.
22 Chhowalla, M., Shin, H.S., Eda, G. et al. (2013). *Nat. Chem.* 5: 263.
23 Wei, Z., Li, B., Xia, C. et al. (2018). *Small Methods* 2: 1800094.
24 Cui, Y., Li, B., Li, J., and Wei, Z. (2017). *Sci. China Phys. Mech. Astron.* 61: 016801.
25 Wang, X., Cui, Y., Li, T. et al. (2019). *Adv. Opt. Mater.* 7: 1801274.
26 Cui, Y., Zhou, Z., Li, T. et al. (2019). *Adv. Funct. Mater.* 29: 1900040.
27 Liu, C.-C., Feng, W., and Yao, Y. (2011). *Phys. Rev. Lett.* 107: 076802.
28 Liu, C.-C., Jiang, H., and Yao, Y. (2011). *Phys. Rev. B* 84: 195430.
29 Osada, M. and Sasaki, T. (2012). *Adv. Mater.* 24: 210.
30 Dean, C.R., Young, A.F., Meric, I. et al. (2010). *Nat. Nanotechnol.* 5: 722.
31 Ashton, M., Paul, J., Sinnott, S.B., and Hennig, R.G. (2017). *Phys. Rev. Lett.* 118: 106101.

32 Mounet, N., Gibertini, M., Schwaller, P. et al. (2018). *Nat. Nanotechnol.* 13: 246.
33 Li, H., Zhang, Q., Duan, X. et al. (2015). *J. Am. Chem. Soc.* 137: 5284.
34 Li, B., Xing, T., Zhong, M. et al. (2017). *Nat. Commun.* 8: 1958.
35 Yu, H., Liao, M., Zhao, W. et al. (2017). *ACS Nano* 11: 12001.
36 Chen, J., Shao, K., Yang, W. et al. (2019). *ACS Appl. Mater. Interfaces* 11: 19381.
37 Yang, Z., Jie, W., Mak, C.-H. et al. (2017). *ACS Nano* 11: 4225.
38 Wang, L., Xu, X., Zhang, L. et al. (2019). *Nature* 570: 91.
39 Zhang, Q., Wang, X.-F., Shen, S.-H. et al. (2019). *Nat. Electron.* 2: 164.